SCIENTIFIC REPORTS

OPEN

SUBJECT AREAS:
IMAGING TECHNIQUES AND AGENTS
BIOMEDICAL MATERIALS
NANOPARTICLES
IMAGING STUDIES

Received
19 June 2014

Accepted
29 October 2014

Published
14 November 2014

Correspondence and requests for materials should be addressed to Y.Z. (zhaoyanli@ntu.edu.sg)

* These authors contributed equally to this work.

"Turn-on" fluorescence probe integrated polymer nanoparticles for sensing biological thiol molecules

Chung Yen Ang[1]*, Si Yu Tan[1]*, Yunpeng Lu[1], Linyi Bai[1], Menghuan Li[2], Peizhou Li[1], Quan Zhang[1], Subramanian Tamil Selvan[3] & Yanli Zhao[1,2]

[1]Division of Chemistry and Biological Chemistry, Nanyang Technological University, 21 Nanyang Link, Singapore 637371, Singapore, [2]School of Materials Science and Engineering, Nanyang Technological University, Singapore 639798, Singapore, [3]Institute of Material Research and Engineering, 3 Research Link, Singapore 117602, Singapore.

A "turn-on" thiol-responsive fluorescence probe was synthesized and integrated into polymeric nanoparticles for sensing intracellular thiols. There is a photo-induced electron transfer process in the off state of the probe, and this process is terminated upon the reaction with thiol compounds. Configuration interaction singles (CIS) calculation was performed to confirm the mechanism of this process. A series of sensing studies were carried out, showing that the probe-integrated nanoparticles were highly selective towards biological thiol compounds over non-thiolated amino acids. Kinetic studies were also performed to investigate the relative reaction rate between the probe and the thiolated amino acids. Subsequently, the Gibbs free energy of the reactions was explored by means of the electrochemical method. Finally, the detection system was employed for sensing intracellular thiols in cancer cells, and the sensing selectivity could be further enhanced with the use of a cancer cell-targeting ligand in the nanoparticles. This development paves a path for the sensing and detection of biological thiols, serving as a potential diagnostic tool in the future.

Thiols in biological systems play a significant role in the maintenance of life. Owing to their oxidative properties, biological thiols serve as antioxidants[1–3], aid in the inhibition of cellular apoptosis[4–7], and participate as scaffolds for the formation of complex three-dimensional protein structures. All of these activities occur through the formation or cleavage of disulfide bond. Among biological thiols, a lot of attention has been given to glutathione (GSH), cysteine (Cys) and homocysteine (Hcy). Exceptionally high concentration of any of these thiol compounds could act as a signal for the abnormality of cells including cancer, cardiovascular disease, AIDS and angiogenesis[8–13]. Therefore, the detection of these thiol-containing compounds is crucial as a form of diagnostics. In view of this fact, various strategies, such as chromatography techniques, nanoparticle (NP) based reporters, and fluorescence assays, have been developed for the detection and sensing of intracellular thiol compounds[14–20]. Of these techniques, the fluorescence assays are often highly favored over other techniques owing to their high selectivity, low cost and simplicity, which can be applied without the use of sophisticated equipment[21]. However, lipophilic nature of these fluorescence probes has greatly reduced their pharmacokinetic properties, and hence their uses for *in vivo* detection and sensing are still far from reach[22]. Furthermore, these probes normally do not possess cancer cell-targeting property, significantly limiting their specificity for *in vivo* applications[23,24]. In this work, we developed a "proof of concept" solution to address these issues by designing a molecular probe and then integrating it into biocompatible polymer based NPs for sensing intracellular thiols. The utilization of the polymer NP carriers could protect potential biodegradation of the molecular probe during the circulation before reaching the target cells. In addition, a folic acid targeting ligand was introduced into the NP system for targeted thiol sensing.

The use of nanocarriers for the delivery of cargoes has shown improved bioavailability of the later significantly in biological systems[25–28]. Recently, we reported the preparation of polyacrylate based NPs (ZG-20 NPs) as a carrier for *in vivo* drug delivery[29]. The ZG-20 NPs were fabricated by a supramolecular self-assembly of β-cyclodextrin (β-CD) conjugated polyacrylic acid (PAA-CD), adamantane (AD) conjugated polyacrylic acid (PAA-AD), and AD conjugated PEG (PEG-AD). Anticancer drug doxorubicin was loaded into the NP system, showing enhanced chemotherapeutic effect as compared with free doxorubicin. In the continuation of this work,

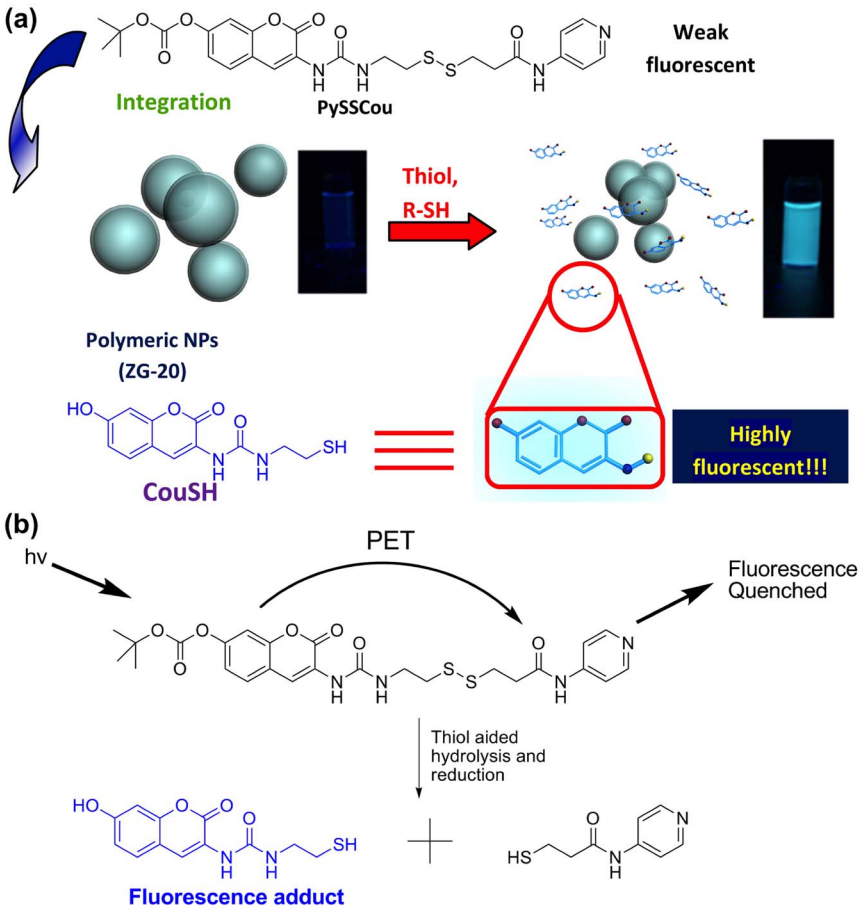

Figure 1 | (A) Supramolecular formation of PySSCou-containing ZG-20 NPs. The chemical structures of the components for the formation of PySSCou-containing ZG-20 NPs are shown in Figure S1. The ZG-20 NPs experience a fluorescence enhancement upon reaction with biological thiol compounds. (B) Schematic illustration of the working principle for the thiol-responsive PySSCou probe.

we herein integrated a "turn-on" thiol-responsive fluorescence probe (PySSCou) into the same NP system for sensing biological thiol compounds (Figure 1A).

The PySSCou molecule was designed as a responsive probe towards thiols. Its main fluorescence signal originates from the coumarin group in the probe. Initially, the fluorescence is mainly suppressed by the pyridine group, which is connected to the coumarin group by a disulfide bond-containing linkage. It was proposed that the pyridine group might quench off the fluorescence of the coumarin group by photoinduced electron transfer (PET) process (Figure 1B)[30,31]. In addition, the pyridine group could form a host-guest complex with β-CD in PAA-CD, thereby facilitating the integration of the probe into the NPs[32]. With this design, the biological thiols can enhance the fluorescence of the ZG-20 NPs by catalyzing the hydrolysis of the carbonate group on the 7th position of the coumarin unit and also the reduction of the disulfide bond in PySSCou to remove the pyridine group from the molecule[33–35]. The removal of the pyridine group inhibits the PET process on the fluorescence probe, hence recovering the fluorescence from the coumarin unit. Although there are several thiol-responsive probes reported in literature[36–44], the integration of a fluorescence probe into a nanocarrier to realize fluorescent thiol sensing has not been investigated so far.

Results

Preparation and characterization of probe-integrated ZG-20 NPs. The PySSCou molecule was synthesized from commercially available starting materials (see Figure S1 and synthetic details in the Supporting Information (SI)). The molecule was dissolved in dimethyl sulfoxide (DMSO) to yield a stock solution, which was then used for the preparation of ZG-20 NPs. In a typical preparation of ZG-20 NPs, 0.1 equiv. of PySSCou was mixed with PAA-AD containing 0.25 equiv. of the AD unit. To this mixture was added with 0.2 equiv. of PEG-AD followed by the addition of 0.1 equiv. of PAA-CD. The mixture was then washed thoroughly with phosphate buffered saline (PBS) so as to ensure that all unbound precursors were removed. Finally, the NPs were re-suspended in PBS for subsequent characterizations and applications.

The size and morphology of the as-prepared ZG-20 NPs were characterized by transmission electron microscope (TEM). The TEM image (Figure 2) shows that the NPs are spherical in shape and have the mean diameter of 18.7 ± 3.8 nm measured from 200 particles. The TEM image also exhibits the absence of large polymeric aggregates, confirming that the NPs were formed under a controlled manner. The surface charge of the NPs was measured using the Zeta potential technique, which was found to be −4.56 mV. The slight negative surface charge may be attributed to the free carboxylate groups on the PAA conjugates. The negatively charged surface of NPs is in favor of minimizing non-specific interactions between the NPs and cells with negatively charged surface.

Photophysical properties of probe-integrated ZG-20 NPs. The UV-Vis spectrum of the ZG-20 NPs shows that the NPs exhibit the maximum absorption at the wavelength of 330 nm (Figure S6 in the SI). Based on this observation, the fluorescence spectrum of the ZG-20 NPs was measured. The NPs exhibit a weak fluorescence signal at 417 nm. In addition, UV-Vis spectroscopic studies reveal that the ZG-20 NPs have a loading capacity of 2.75 w/w% for the

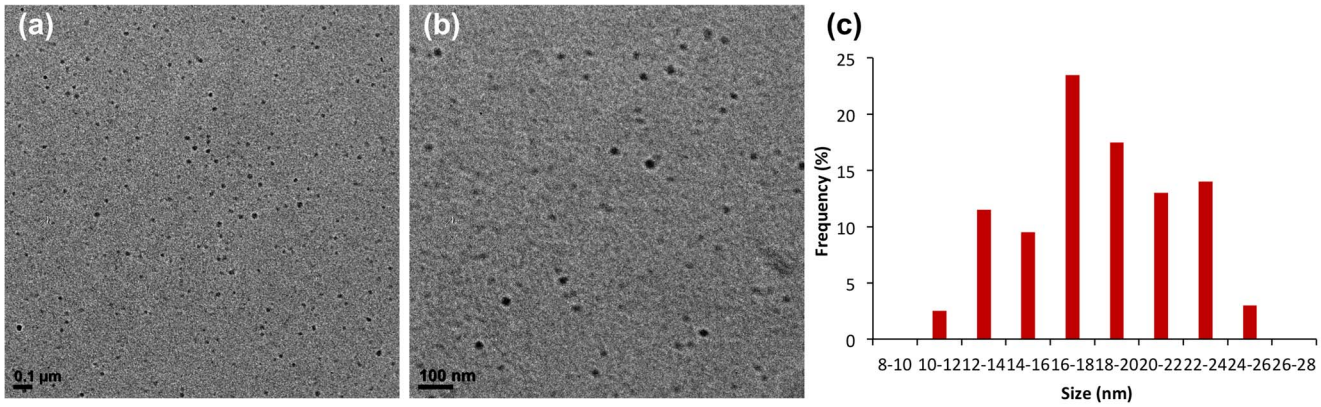

Figure 2 | (A) TEM image and (B) Zoomed-in TEM image of ZG-20 NPs. (C) Histogram showing the size distribution of ZG-20 NPs measured from 200 NPs from TEM image.

PySSCou probe molecule (see Section 7 in the SI). The XPS (X-ray photoelectron spectroscopy) measurement also indicates that the NPs contain 2.65 mol% of S relative to N and C elements (Figure S10 in the SI). These measurements confirmed that the PySSCou molecule was successfully integrated into the polymeric NP system, as the NPs without the PySSCou loading did not exhibit these properties. Thus, the NP system could serve as a host for effective loading of the PySSCou molecule.

Detection selectivity. The detection selectivity of probe-integrated ZG-20 NPs was evaluated by conducting the co-incubation of the NPs (0.66 mg mL^{-1}) with various amino acids and thiol compounds (5.0 mM) in PBS buffer overnight. In this study, we used dithiolthretol (DTT) to investigate the response of the NP system. Although DTT is not considered as a biological thiol compound, it is a well-known thiolated reducing agent and could serve as a positive control for comparison. After the overnight incubation, we measured the fluorescence intensity of the NP solution at 477 nm under the excitation wavelength of 330 nm. The measurement results show that the ZG-20 NPs possess an excellent selectivity, *i.e.*, the NPs only respond to various thiol compounds but not to the non-thiolated amino acids (Figure 3A). Similarly, the selectivity experiments of the naked PySSCou molecule with these amino acids and thiol compounds also show the same trend, thereby confirming that the integration of PySSCou into the polymeric NPs did not compromise its selectivity (Figure S5 in the SI).

Detection limit determination. In order to study the sensitivity of the NP system, its response upon changing the concentration of Cys was recorded. It was observed that the response decreased with the decrease in the Cys concentration (Figure 3B). By using the same set of experiment data, the plot of the intensity at the maximum wavelength (477 nm) versus the Cys concentration gave a linear relationship between the two variables (Figure S7 in the SI). The detection limit (5.75 μM) of the NP system was obtained based on the linear plot.

Quantum yield calculation. In the design of the fluorescence probe, we proposed that the reaction of the integrated probe with thiol compounds could release highly fluorescent coumarin molecule (CouSH) into the testing buffer. In order to confirm this mechanism, we measured the quantum yields of PySSCou as well as its coumarin product CouSH after reaction with DTT (see Section 6 in the SI for details). The measurement results reveal that the corresponding quantum yields increased from 1.0% to 12.0%, indicating that the reaction released highly fluorescent CouSH into solution in order to serve as a signal for the sensing application. We also performed the GC EI-MS (gas chromatography electron ionization–mass spectrometry) analysis of DTT-treated NP solution (Figure S11 in the SI). The GC EI-MS analysis shows the presence of an m/z value at 281, corresponding to the $[M+H]^+$ peak of the released CouSH molecule.

Kinetic studies. In order to further probe the reaction kinetics of NPs with various thiol compounds, we carried out the time-dependent fluorescence measurements of the NP solution with the incubation of various thiols at pH 7.4 and 37°C over a period of 3 h (Figure 4A). The results of the kinetic experiments show that the treatment of the NPs with various thiol compounds induces the enhancement of the fluorescence at 477 nm under the excitation of 330 nm. DTT led to the highest rate of response, followed by Cys, Hcy and GSH. In addition, a blank run where no additive was added into the NP solution during the incubation period was performed as a control. In the control case, there was no increase in the fluorescence intensity at 477 nm over 3 h, while a decrease in the fluorescence intensity was observed. We speculated that the decrease in the fluorescence intensity was a result of the hydrolysis of the carbonate group on the 7^{th} position of the coumarin molecule. In the initial state, electron-withdrawing carbonate group exhibits an inductive effect on the PySSCou molecule, contributing to the slight inhibition of the PET process to the pyridine group. The unstable carbonate group is prone to hydrolyze, converting into electron-donating phenoxide anion. The resulted phenoxide anion further promotes the PET process, which leads to the decrease of the fluorescence for the blank experiment. The presence of the carbonate group in the PySSCou molecule has two reasons. One is for synthesis reason that the incorporation of the carbonate group prevents the nucleophilic attack of the phenoxide group onto the 4-nitrophenyl chloroformate unit. The second reason is to employ it as a normalization signal during all the kinetic studies. It was observed from the kinetic studies that all the kinetic curves begin at the same starting point, having absolute fluorescence intensity at about 40 a.u. This observation indicates that all the kinetic experiments were conducted with the same initial NP concentration. At the end of the kinetic experiments, the fluorescence spectra of the NPs were recorded under the excitation wavelength of 330 nm (Figure 4B). Initially quenched fluorescence of probe-integrated NPs showed a fluorescence enhancement upon the reactions with various thiol compounds. In addition, kinetic studies were also performed using the naked PySSCou molecule and a same trend of reactivity was observed (Figure S4 in the SI).

Electrochemical and Gibbs free energy measurements. We then carried out the cyclic voltammetry (CV) measurements of PySSCou and thiol compounds in order to work out their reduction potentials and subsequently to estimate the Gibbs free

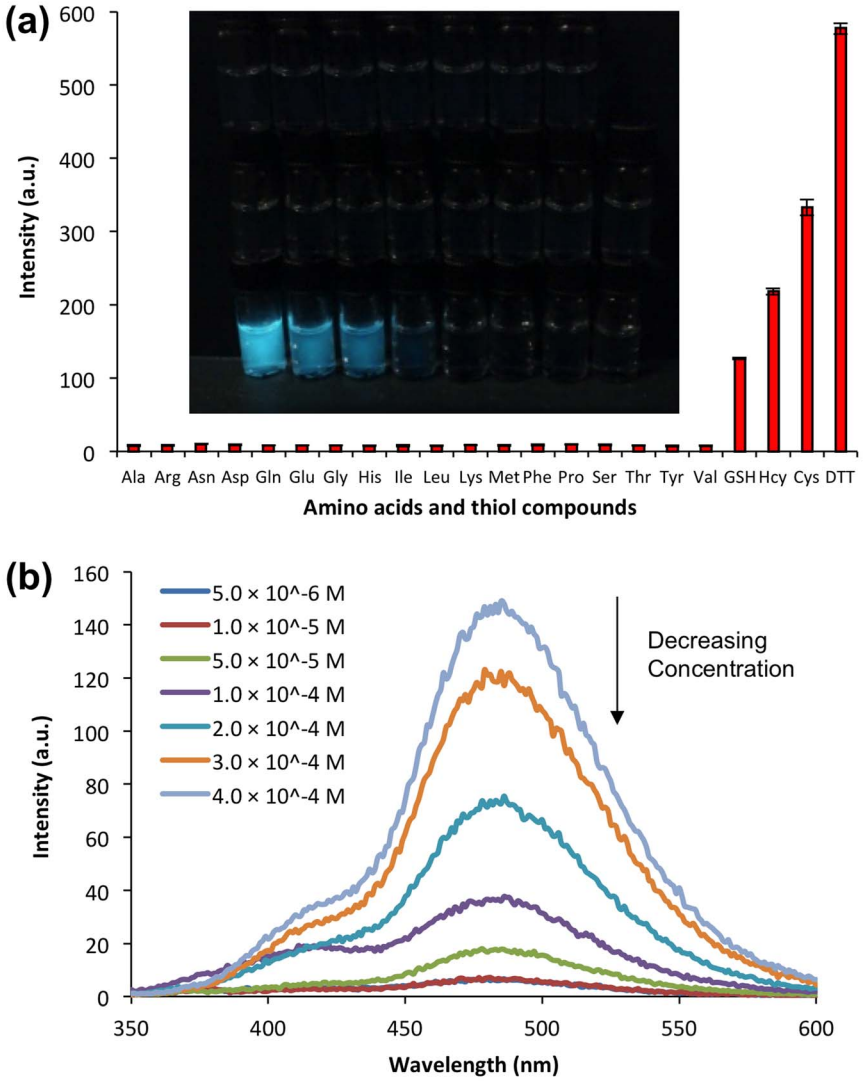

Figure 3 | (A) Fluorescence intensity (λ = 477 nm) of ZG-20 NPs after overnight co-incubation with various amino acids and thiol compounds (5.0 mM) in PBS (pH = 7.4) at 37°C (λ_{ex} = 330 nm). Error bar: n = 3. Inset: Fluorescence images of the resulted NP solutions under UV lamp. From bottom left to top right: ZG-20 NPs treated with DTT, Cys, Hcy, GSH, Methionine (Met), Alanine (Ala), Glycine (Gly), Leucine (Leu), Histidine (His), Isoleucine (Ile), Tryptophan (Trp), Tyrosine (Tyr), Aspartic acid (Asp), Arginine (Arg), Asparagine (Asn), Lysine (Lys), Phenylalanine (Phe), Threonine (Thr), Proline (Pro), Serine (Ser), Valine (Val), Glutamine (Gln) and Glutamic acid (Glu). (B) Fluorescence spectra of the NP solution after overnight co-incubation with various concentrations of Cys in PBS (pH = 7.4) at 37°C.

energy of the reactions (Table 1). The Gibbs free energy estimation indicates that all the thiol compounds could react with PySSCou spontaneously. It was observed that the trend in the Gibbs free energy agrees with the trend obtained from the kinetic experiments.

Computation studies for the confirmation of PET mechanism. Computational studies were performed to determine the orbital diagram of the possible transition during photo-excitation[30,45]. Density functional theory (DFT) was employed to optimize the hydrolyzed PySSCou with the hydrogen bonded water using the basis set of B3LYP/6-311++G (d,p) on the suit of Gaussian 09 W program. Upon the optimization of the geometry, the configuration interaction singles (CIS) were performed to calculate the transition to the excited state[46]. The calculation results reveal that the S0 to S1 transition has the highest oscillation strength as compared to other excited states. From the analysis of the S1 excited state, we found that one of the transitions was contributed by the transition from the HOMO to the LUMO + 10 orbitals. As shown in Figure 5A, the HOMO orbital has the majority of the electron density localized on the coumarin moiety, while the LUMO + 10 orbital has its electron stretched from the coumarin moiety to the pyridine group. Such a difference in the localization of the electron density confirms that the intramolecular PET process occurs with the direction of PET starting from the coumarin moiety to the pyridine group. A similar calculation was carried out on hydrogen bonded CouSH (Figure 5B). The CIS calculation results show that the S0 to S1 transition has the highest oscillation strength with the only contribution from the HOMO to LUMO + 6 orbitals. From the similar analysis of the orbital diagrams, it was observed that the electron densities were mainly localized on the coumarin moiety. These calculation results confirm that the cleavage of the disulfide bond terminates the intramolecular PET process, hence recovering the fluorescence.

Targeted intracellular imaging of biological thiols. In order to assess the bio-applicability of the probe-integrated ZG-20 NPs for intracellular sensing of thiol compounds, two types of ZG-20 NPs were prepared. One of them (FA+VE ZG-20 NPs) was integrated with the AD conjugated folic acid (FA-AD), while the other one (FA–VE ZG-20 NPs) did not contain FA-AD. In our previous work, we

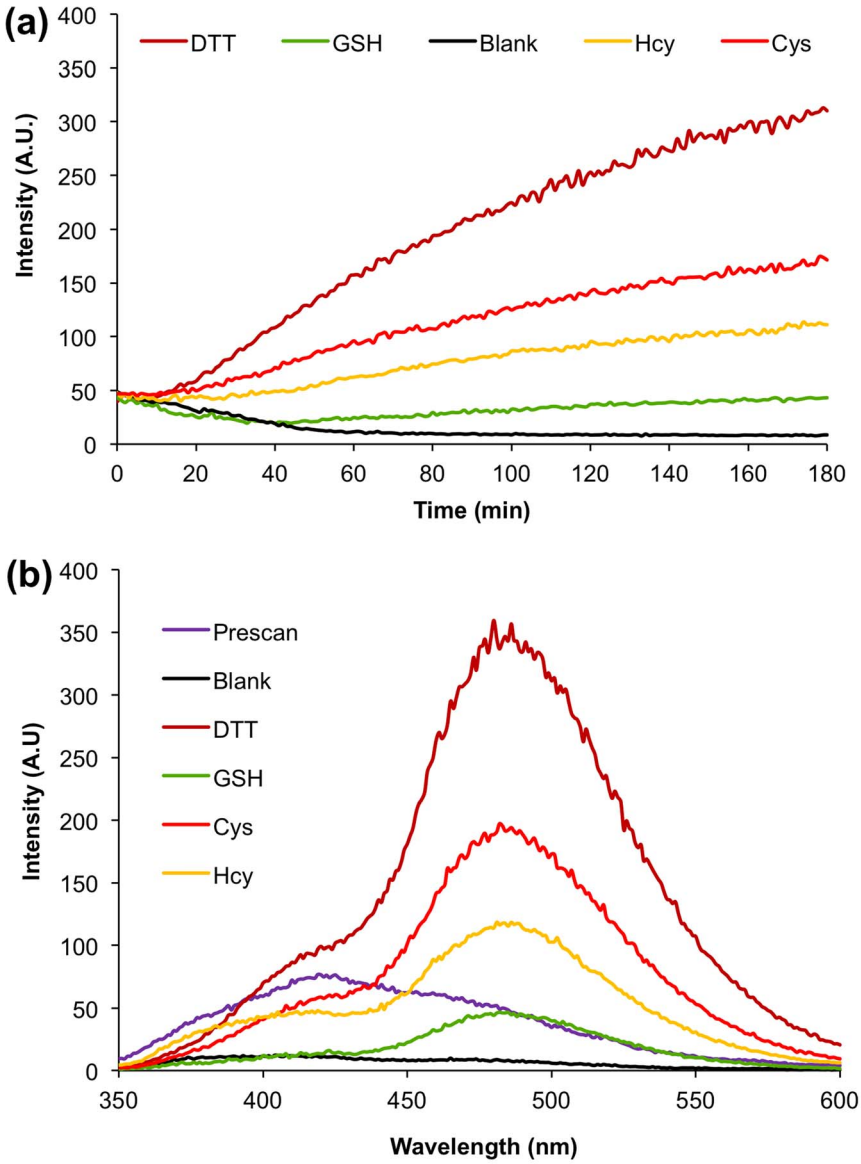

Figure 4 | (A) Kinetic measurements of the ZG-20 NPs with and without (Blank) various thiol compounds. λ_{ex} = 330 nm, λ_{em} = 477 nm. (B) Fluorescence spectra of ZG-20 NPs (λ_{ex} = 330 nm) after incubation with and without (Blank) various thiol compounds (5 mM). Prescan curve refers to the fluorescence spectrum of the NPs before the incubation, and Blank curve means that the fluorescence spectrum of the NPs was recorded after the same incubation time without the addition of thiol compounds.

have demonstrated that the integration of FA-AD into the NPs could induce the folate mediated endocytosis of the PAA NPs by cancer cells[29]. Hence, we would like to prove that the sensing of intracellular thiols could also be highly selective through the introduction of a targeting ligand into the NP system. The two types of NPs were incubated with a pre-cultured B16-F10 mouse melanoma cells followed by taking the fluorescence microscopy images of the cells. From the fluorescence microscopy images (Figure 6), it was observed that the cells treated with the FA+VE ZG-20 NPs show a positive fluorescence signal (blue color), particularly within the cytoplasm of the cells. However, the same experiment conducted using the FA–VE ZG-20 NPs exhibit the absence of the fluorescence signal. These experiment results indicate that the selectivity of the probe can be altered by the conjugation of folate group on the NPs.

Table 1 | Summary of the results from the electrochemical analysis. All potentials reported were measured against the Ag/AgCl electrode

	PySSCou	Cys	DTT	GSH	Hcy
E_{ox} [V]	−0.590	−0.869	0.360	−0.565	−0.589
E_{red} [V]	−1.010	−1.080	−3.690	−1.050	−1.030
$E°_{1/2}$ [V]	−0.805	−0.975	−1.665	−0.808	−0.810
$E°_{Cell}$ [a] [V]	0	0.170	0.860	0.003	0.005
$\Delta G°$ [b] [J/mol]	0	−2900	−15000	−51	−87

a) Difference between the standard reduction potentials ($E°_{1/2}$) of PySSCou and respective thiol compounds. b) Estimated Gibbs free energy based on $\Delta G° = -nFE°_{cell}$, where n is the number of electrons involved (2 electrons for disulfide exchange reaction) and F is Faraday's constant.

It is known that cancer cells exhibit higher intracellular thiol concentration, and non-cancerous cells express a low amount of thiol compounds in the intracellular environment. Thus, non-specific targeting of NPs may provide false positive results during the cancer imaging. In addition, the fluorescence images of the cells upon the incubation with the naked PySSCou molecule were recorded. In this control experiment, no fluorescence from the treated cells was observed. This observation agrees with the literature report that free dye molecules have certain difficulties in the trans-membrane

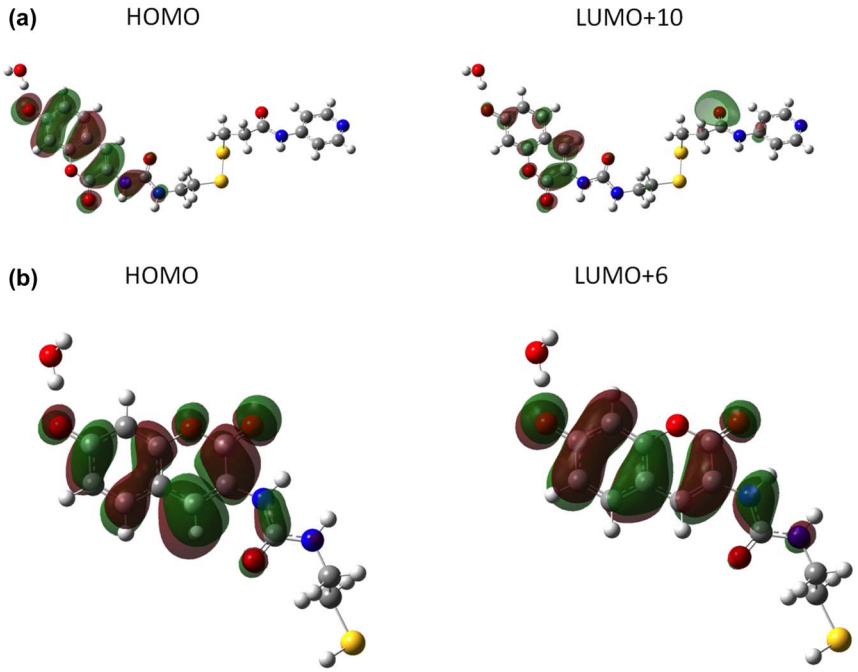

Figure 5 | Frontier molecular orbitals (MO) diagrams of A) PySSCou (HOMO and LUMO + 10) and B) CouSH (HOMO and LUMO + 6).

trafficking process[47]. The control experiment confirms that the folate-containing NPs have the ability to carry the PySSCou probe into the intracellular environment. Furthermore, we conducted the MTT (3-(4,5-dimethylthiazol-2-yl)-2,5-diphenyltetrazolium bromide) cytotoxicity assay for the cells treated with the probe-integrated NPs and the naked PySSCou molecule. The experiments showed that the NPs exhibit insignificant toxicity to the cells under the concentrations measured (Figure S17 in the SI), demonstrating their suitability for biological applications. Thus, the application of the NPs for intracellular sensing of thiol compounds was successfully demonstrated.

Discussion

By utilizing the intramolecular PET mechanism, we rationally designed and synthesized a coumarin based "turn-on" fluorescence probe that consists of a disulfide bond connected to a quencher. The pyridine moiety in the PySSCou probe not only serves as an electron reservoir for the quenching of the coumarin fluorescence, but also

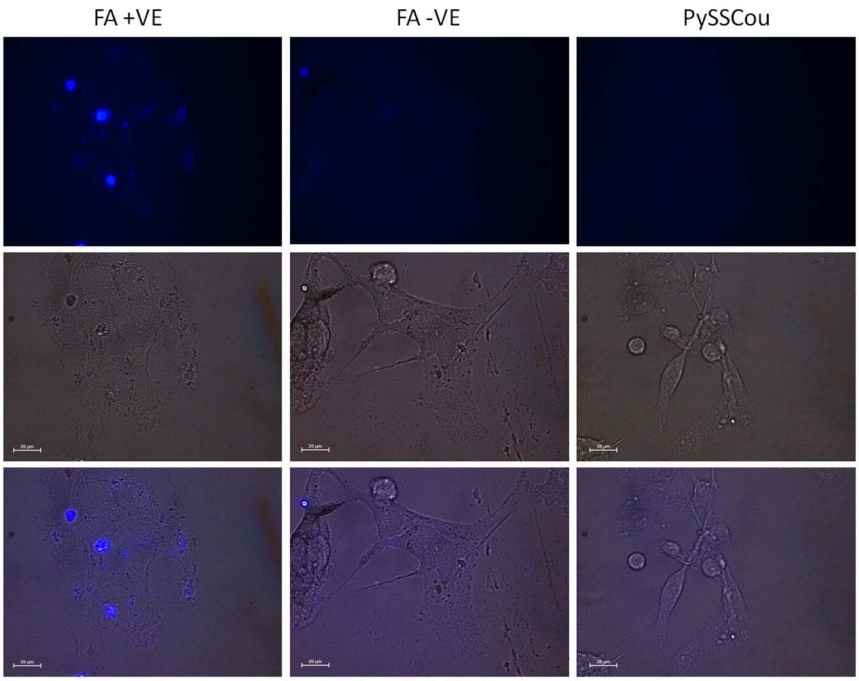

Figure 6 | Fluorescence microscopy images of B16-F10 cells after co-incubation with FA+VE ZG-20 NPs, FA–VE ZG-20 NPs, and PySSCou molecule. Upper three: Fluorescence images were taken in the DAPI (4′,6-diamidino-2-phenylindole) channel. Excitation filter: 350/50 nm and emission filter: 460/50 nm. Middle three: Bright field images of the respective cells. Bottom three: Merged images of the respective bright field and fluorescence cell images. Scale bar is 20 μm.

allows easy integration of the probe into polymeric NPs for *in vitro* sensing of biological thiol molecules. To confirm the presence of the PySSCou probe in the polymeric NPs, various characterization techniques such as XPS and UV-Vis spectroscopy were employed. The characterization results proved that the PySSCou probe was indeed incorporated into the polymeric NPs. Together with our previous work on the loading and delivery of doxorubicin using this NP system, the research demonstrated the versatility of the NP system for the integration of different cargos capable of multiple uses.

In terms of the selectivity towards the thiol compounds, the disulfide bond on PySSCou enables the probe to react with thiols in a highly selective manner, which was proven by a series of control experiments against the non-thiolated amino acids. The electrochemical studies confirmed that the reaction between biological thiols and PySSCou was a spontaneous process with a negative Gibbs free energy. In addition, various *in vitro* thiol detection studies showed that the probe, either as a free molecule or being integrated into the NPs, could present excellent responses to biological thiol compounds, concluding that the integration process does not influence the selectivity and reactivity of the probe. On the other hand, this NP system allows for the incorporation of cancer cell-targeting ligand for enhancing the sensing selectivity to the intracellular thiol compounds within cancerous cells.

In conclusion, we have successfully developed a novel "turn-on" fluorescence probe that has been integrated into polymeric NPs for sensing applications. The as-prepared NPs have the capability to respond to various biological thiol compounds against the non-thiolated amino acids. Intracellular sensing of biological thiols in B16-F10 mouse melanoma cells using the probe-integrated NPs has been carried out, indicating that the sensitivity and selectivity of the NPs could be altered by the integration of the targeting ligand. In addition, computational studies have been performed to prove that the initial fluorescence quenching of the probe is a result of intramolecular PET process. The PET process could be terminated upon the reductive cleavage of the disulfide bond within the probe molecule by the endogenous biological thiols, confirming the "turn-on" process of the probe. Since the NP system has the capability to selectively deliver the cargoes into the tumor sites in tumor-bearing nude mouse models[29], the probe-integrated NPs show a promising potential to be utilized in the sensing of biological thiol compounds *in vivo*.

Methods

Preparation of NPs. Prior to the preparation of NPs, all components were prepared as stock solutions in their respective concentrations. PAA-CD: 8.6 mg/mL in water, PAA-AD: 26.0 mg/mL in DMSO, PEG-AD: 16.8 mg/mL in water, PySSCou: 11.7 mM in DMSO, and FA-AD: 11.7 mM in DMSO.

Preparation of ZG-20 NPs or FA-VE ZG-20 NPs. PAA-AD solution (4 μL) was added with PEG-AD solution (66 μL) and PySSCou solution (12 μL). The mixture was stirred thoroughly before the addition of PAA-CD solution (66 μL) and PBS (1 mL). The mixture was sonicated for 15 min and the NPs formed were isolated by high speed centrifugation. The supernatant was discarded and the NPs were re-dispersed in PBS (1 mL). The NPs were again isolated by high speed centrifugation and the process was repeated for two addition cycles to ensure the thorough washing of the NPs. Finally, the NPs were re-dispersed either in PBS (3 mL) to achieve a concentration of 0.66 mg/mL for fluorescence and kinetic measurements or in PBS (0.3 mL) to achieve a concentration of 6.6 mg/mL for bioimaging experiments.

Preparation of FA+VE ZG-20 NPs. The procedure for the preparation of FA+VE ZG-20 NPs was similar to the preparation of FA-VE ZG-20 NPs, while adding the FA-AD solution (12 μL) to the mixture prior to the addition of PAA-CD solution. The washed NPs were re-dispersed in PBS (0.3 mL) for bioimaging experiments.

Computational Studies. All computational studies were performed using the Gaussian 09 W program. DFT calculation was performed for the optimization of the molecules using the basis set of B3LYP/6-311++G (d,p). The polarization continuum model using the integration formalism variant (IEFPCM) with water as solvent was included in the optimization process. The CIS calculations of the excited states were also conducted with the same basis set.

Intracellular Sensing and Cytotoxicity Studies. Intracellular sensing of biological thiol compounds was conducted on mouse melanoma B16-F10 cells. In a typical imaging experiment, 8.0 × 104 cells were seeded into a SPL 200350 coverglass-bottom dish and the cells were incubated overnight. Thereafter, FA-VE ZG-20 NP solution or FA+VE ZG-20 NP solution (200 μL, 1.0 mg/mL) was added, and the cells were then incubated overnight. The medium was removed. The cells were washed 3 times with PBS and then added with fresh medium prior to imaging.

In the MTT cytotoxicity assay, the cells were first seeded into a 96 well plates at a seeding density of 1.0 × 104 cells per well prior to overnight incubation. Thereafter, 10 μL per well of FA+VE ZG-20 NPs or PySSCou in PBS with various concentrations were added and followed by a further overnight incubation. The medium was removed and replaced by 100 μL per well of fresh medium containing 0.5 mg mL-1 of MTT. The cells were returned to the incubator for 4 h before removing the medium again. The residual purple crystal was dissolved in DMSO (100 μL per well) and the absorbance of the purple solution was measured at 562 nm using a plate reader (Infinite® 200 PRO plate reader). The viability of each well was determined as a relative percentage to the control well where only water was added. Each data was reported as a mean of eight replicates and the error bars were the results of the standard deviations of these replicates.

Detailed synthesis, methods, and characterization data are presented in the supporting information.

1. Pompella, A., Visvikis, A., Paolicchi, A., De Tata, V. & Casini, A. F. The changing faces of glutathione, a cellular protagonist. *Biochem. Pharmacol.* **66**, 1499–1503 (2003).
2. Deneke, S. M. Thiol-based antioxidants. *Curr. Top. Cell. Regul.* **36**, 151–180 (2000).
3. Chae, H. Z., Uhm, T. B. & Rhee, S. G. Dimerization of thiol-specific antioxidant and the essential role of cysteine-47. *Proc. Natl. Acad. Sci. U.S.A.* **91**, 7022–7026 (1994).
4. Sandstrom, P. A., Mannie, M. D. & Buttke, T. M. Inhibition of activation-induced death in t-cell hybridomas by thiol antioxidants - oxidative stress as a mediator of apoptosis. *J. Leukocyte Biol.* **55**, 221–226 (1994).
5. Sato, N. *et al.* Thiol-mediated redox regulation of apoptosis - possible roles of cellular cellular thiols other than glutathione in t-cell apoptosis. *J. Immunol.* **154**, 3194–3203 (1995).
6. Watson, R. W. G., Rotstein, O. D., Nathens, A. B., Dackiw, A. P. B. & Marshall, J. C. Thiol-mediated redox regulation of neutrophil apoptosis. *Surgery* **120**, 150–158 (1996).
7. Stefan, C. *et al.* Mechanism of dithiocarbamate inhibition of apoptosis: Thiol oxidation by dithiocarbamate disulfides directly inhibits processing of the caspase-3 proenzyme. *Chem. Res. Toxicol.* **10**, 636–643 (1997).
8. Schirmer, R. H., Muller, J. G. & Krauthsiegel, R. L. Disulfide-reductase inhibitors as chemotherapeutic-agents - the design of drugs for trypanosomiasis and malaria. *Angew. Chem. Int. Ed. Engl.* **34**, 141–154 (1995).
9. Seshadri, S. *et al.* Plasma homocysteine as a risk factor for dementia and alzheimer's disease. *N. Engl. J. Med.* **346**, 476–483 (2002).
10. Zhang, S., Ong, C. N. & Shen, H. M. Critical roles of intracellular thiols and calcium in parthenolide-induced apoptosis in human colorectal cancer cells. *Cancer Lett.* **208**, 143–153 (2004).
11. Krauth-Siegel, R. L., Bauer, H. & Schirmer, H. Dithiol proteins as guardians of the intracellular redox milieu in parasites: Old and new drug targets in trypanosomes and malaria-causing plasmodia. *Angew. Chem. Int. Ed.* **44**, 690–715 (2005).
12. Wadhwa, S. & Mumper, R. J. D-penicillamine and other low molecular weight thiols: Review of anticancer effects and related mechanisms. *Cancer Lett.* **337**, 8–21 (2013).
13. Refsum, H., Ueland, P. M., Nygard, O. & Vollset, S. E. Homocysteine and cardiovascular disease. *Annu. Rev. Med.* **49**, 31–62 (1998).
14. Newton, G. L., Dorian, R. & Fahey, R. C. Analysis of biological thiols - derivatization with monobromobimane and separation by reverse-phase high-performance liquid-chromatography. *Anal. Biochem.* **114**, 383–387 (1981).
15. Richie, J. P. & Lang, C. A. The determination of glutathione, cyst(e)ine, and other thiols and disulfides in biological samples using high-performance liquid-chromatography with dual electrochemical detection. *Anal. Biochem.* **163**, 9–15 (1987).
16. Araki, A. & Sako, Y. Determination of free and total homocysteine in human-plasma by high-performance liquid-chromatography with fluorescence detection. *J. Chromatogr. B Biomed. Sci. Appl.* **422**, 43–52 (1987).
17. Lee, J. S., Ulmann, P. A., Han, M. S. & Mirkin, C. A. A DNA-gold nanoparticle-based colorimetric competition assay for the detection of cysteine. *Nano Lett.* **8**, 529–533 (2008).
18. Shang, L. *et al.* Fluorescent conjugated polymer-stabilized gold nanoparticles for sensitive and selective detection of cysteine. *J. Phys. Chem. C* **111**, 13414–13417 (2007).
19. Sudeep, P. K., Joseph, S. T. S. & Thomas, K. G. Selective detection of cysteine and glutathione using gold nanorods. *J. Am. Chem. Soc.* **127**, 6516–6517 (2005).
20. Zhang, F. X. *et al.* Colorimetric detection of thiol-containing amino acids using gold nanoparticles. *Analyst* **127**, 462–465 (2002).
21. Wei, W., Liang, X. J., Hu, G. Z., Guo, Y. & Shao, S. J. A highly selective colorimetric probe based on 2,2′,2″-trisindolylmethene for cysteine/homocysteine. *Tetrahedron Lett.* **52**, 1422–1425 (2011).

22. Kobayashi, H., Ogawa, M., Alford, R., Choyke, P. L. & Urano, Y. New strategies for fluorescent probe design in medical diagnostic imaging. *Chem. Rev.* **110**, 2620–2640 (2010).
23. Moon, W. K. *et al.* Enhanced tumor detection using a folate receptor-targeted near-infrared fluorochrome conjugate. *Bioconjugate Chem.* **14**, 539–545 (2003).
24. Tung, C. H., Lin, Y. H., Moon, W. K. & Weissleder, R. A receptor-targeted near-infrared fluorescence probe for *in vivo* tumor imaging. *ChemBioChem* **3**, 784–786 (2002).
25. Ang, C. Y., Tan, S. Y. & Zhao, Y. Recent advancements of biocompatible nanocarriers for delivery of chemotherapeutic cargoes towards cancer therapy. *Org. Biomol. Chem.* **12**, 4776–4806 (2014).
26. Torchilin, V. P. Multifunctional nanocarriers. *Adv. Drug Delivery Rev.* **64**, 302–315 (2012).
27. Ganta, S., Devalapally, H., Shahiwala, A. & Amiji, M. A review of stimuli-responsive nanocarriers for drug and gene delivery. *J. Control. Release* **126**, 187–204 (2008).
28. Ding, M. M. *et al.* Toward the next-generation nanomedicines: Design of multifunctional multiblock polyurethanes for effective cancer treatment. *ACS Nano* **7**, 1918–1928 (2013).
29. Ang, C. Y. *et al.* Supramolecular nanoparticle carriers self-assembled from cyclodextrin- and adamantane-functionalized polyacrylates for tumor-targeted drug delivery. *J. Mater. Chem. B* **2**, 1879–1890 (2014).
30. Jung, H. S. *et al.* A cysteine-selective fluorescent probe for the cellular detection of cysteine. *Biomaterials* **33**, 945–953 (2012).
31. Yi, L. *et al.* A highly sensitive fluorescence probe for fast thiol-quantification assay of glutathione reductase. *Angew. Chem. Int. Ed.* **48**, 4034–4037 (2009).
32. Baer, A. J. & Macartney, D. H. Alpha- and beta-cyclodextrin rotaxanes of mu-bis(4-pyridyl)bis pentacyanoferrate(ii) complexes. *Inorg. Chem.* **39**, 1410–1417 (2000).
33. Gilbert, H. F. Thiol/disulfide exchange equilibria and disulfide bond stability. *Methods Enzymol.* **251**, 8–28 (1995).
34. Zhang, Q. *et al.* Multifunctional mesoporous silica nanoparticles for cancer-targeted and controlled drug delivery. *Adv. Funct. Mater.* **22**, 5144–5156 (2012).
35. Zhang, Q. *et al.* Biocompatible, uniform, and redispersible mesoporous silica nanoparticles for cancer-targeted drug delivery *in vivo*. *Adv. Funct. Mater.* **24**, 2450–2461 (2013).
36. Jung, H. S., Chen, X. Q., Kim, J. S. & Yoon, J. Recent progress in luminescent and colorimetric chemosensors for detection of thiols. *Chem. Soc. Rev.* **42**, 6019–6031 (2013).
37. Yin, C. X. *et al.* Thiol-addition reactions and their applications in thiol recognition. *Chem. Soc. Rev.* **42**, 6032–6059 (2013).
38. Chen, X., Zhou, Y., Peng, X. J. & Yoon, J. Fluorescent and colorimetric probes for detection of thiols. *Chem. Soc. Rev.* **39**, 2120–2135 (2010).
39. Guo, H. *et al.* Highly selective fluorescent off-on thiol probes based on dyads of bodipy and potent intramolecular electron sink 2,4-dinitrobenzenesulfonyl subunits. *Org. Biomol. Chem.* **9**, 3844–3853 (2011).
40. Jiang, W., Fu, Q., Fan, H., Ho, J. & Wang, W. A highly selective fluorescent probe for thiophenols. *Angew. Chem. Int. Ed.* **46**, 8445–8448 (2007).
41. Tang, B. *et al.* A rhodamine-based fluorescent probe containing a Se-N bond for detecting thiols and its application in living cells. *J. Am. Chem. Soc.* **129**, 11666–11667 (2007).
42. Wang, R., Chen, L., Liu, P., Zhang, Q. & Wang, Y. Sensitive near-infrared fluorescent probes for thiols based on Se-N bond cleavage: Imaging in living cells and tissues. *Chem. Eur. J.* **18**, 11343–11349 (2012).
43. Huang, S.-T., Ting, K.-N. & Wang, K.-L. Development of a long-wavelength fluorescent probe based on quinone–methide-type reaction to detect physiologically significant thiols. *Anal. Chim. Acta* **620**, 120–126 (2008).
44. Qu, L. *et al.* A maleimide-based thiol fluorescent probe and its application for bioimaging. *Sensor Actuat. B - Chem.* **195**, 246–251 (2014).
45. Zhao, G. J., Liu, J. Y., Zhou, L. C. & Han, K. L. Site-selective photoinduced electron transfer from alcoholic solvents to the chromophore facilitated by hydrogen bonding: A new fluorescence quenching mechanism. *J. Phys. Chem. B* **111**, 8940–8945 (2007).
46. Jacquemin, D. *et al.* The geometries, absorption and fluorescence wavelengths of solvated fluorescent coumarins: A cis and td-dft comparative. *Chem. Phys. Lett.* **438**, 208–212 (2007).
47. Becker, A. *et al.* Receptor-targeted optical imaging of tumors with near-infrared fluorescent ligands. *Nat. Biotechnol.* **19**, 327–331 (2001).

Acknowledgments

This research is supported by the National Research Foundation (NRF), Prime Minister's Office, Singapore under its NRF Fellowship (NRF2009NRF-RF001-015) and Campus for Research Excellence and Technological Enterprise (CREATE) Programme–Singapore Peking University Research Centre for a Sustainable Low-Carbon Future, and the NTU-A*Star Centre of Excellence for Silicon Technologies (A*Star SERC No.: 112 351 0003).

Author contributions

C.Y.A. and S.Y.T. designed and conducted the experiments. Y.P.L. conducted the computational studies. L.Y.B. performed the electrochemical studies. M.H.L. and P.Z.L. carried out the characterization of the materials. Q.Z. and S.T.S participated in the experiments and discussions. C.Y.A., S.Y.T. and Y.L.Z. discussed and analyzed the results and jointly wrote the paper.

Additional information

Supplementary information accompanies this paper at http://www.nature.com/scientificreports

Competing financial interests: The authors declare no competing financial interests.

How to cite this article: Ang, C.Y. *et al.* "Turn-on" fluorescence probe integrated polymer nanoparticles for sensing biological thiol molecules. *Sci. Rep.* **4**, 7057; DOI:10.1038/srep07057 (2014).